ACCOUNTS
of chemical research

Subunit Architecture of Intact Protein Complexes from Mass Spectrometry and Homology Modeling†

THOMAS TAVERNER,[§] HELENA HERNÁNDEZ,[§] MICHAL SHARON,[§] BRANDON T. RUOTOLO,[§] DIJANA MATAK-VINKOVIĆ, DAMIEN DEVOS,[‡] ROBERT B. RUSSELL,[‡] AND CAROL V. ROBINSON*[,§]

[§]*Department of Chemistry, Lensfield Road, University of Cambridge, Cambridge CB2 1EW, U.K.,* [‡]*EMBL, Meyerhofstrasse 1, 69177 Heidelberg, Germany*

RECEIVED ON OCTOBER 1, 2007

CONSPECTUS

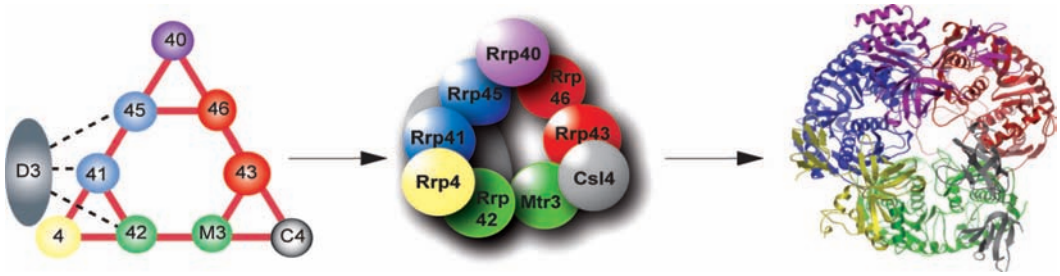

Proteomic studies have yielded detailed lists of protein components. Relatively little is known, however, of interactions between proteins or of their spatial arrangement. To bridge this gap, we are developing a mass spectrometry approach based on intact protein complexes. By studying intact complexes, we show that we are able to not only determine the stoichiometry of all subunits present but also deduce interaction maps and topological arrangements of subunits.

To construct an interaction network, we use tandem mass spectrometry to define peripheral subunits and partial denaturation in solution to generate series of subcomplexes. These subcomplexes are subsequently assigned using tandem mass spectrometry. To facilitate this assignment process, we have developed an iterative search algorithm (SUMMIT) to both assign protein subcomplexes and generate protein interaction networks. This software package not only allows us to construct the subunit architecture of protein assemblies but also allows us to explore the limitations and potential of our approach. Using series of hypothetical complexes, generated at random from protein assemblies containing between six and fourteen subunits, we highlight the significance of tandem mass spectrometry for defining subunits present. We also demonstrate the importance of pairwise interactions and the optimal numbers of subcomplexes required to assign networks with up to fourteen subunits.

To illustrate application of our approach, we describe the overall architecture of two endogenous protein assemblies isolated from yeast at natural expression levels, the 19S proteasome lid and the RNA exosome. In constructing our models, we did not consider previous electron microscopy images but rather deduced the subunit architecture from series of subcomplexes and our network algorithm. The results show that the proteasome lid complex consists of a bicluster with two tetrameric lobes. The exosome lid, by contrast, is a six-membered ring with three additional bridging subunits that confer stability to the ring and with a large subunit located at the base. Significantly, by combining data from MS and homology modeling, we were able to construct an atomic model of the yeast exosome.

In summary, the architectural and atomic models of both protein complexes described here have been produced in advance of high-resolution structural data and as such provide an initial model for testing hypotheses and planning future experiments. In the case of the yeast exosome, the atomic model is validated by comparison with the atomic structure from X-ray diffraction of crystals of the reconstituted human exosome, which is homologous to that of the yeast. Overall therefore this mass spectrometry and homology modeling approach has given significant insight into the structure of two previously intractable protein complexes and as such has broad application in structural biology.

Published on the Web 03/04/2008 www.pubs.acs.org/acr
10.1021/ar700218q CCC: $40.75

Introduction

Many cellular processes are performed by stable protein complexes, and recent predictions have estimated that up to 80% of the yeast proteome exists in complexes with an average of 5.26 proteins.[1] Using tandem-affinity purification (TAP) and mass spectrometry (MS) to identify all proteins associated with a particular TAP fusion protein, researchers have now purified several hundred putative complexes from yeast. Common to all these investigations is the use of standard proteomics in which individual proteins are separated, typically on a 1D gel, and mass spectra of tryptic peptides are used to identify proteins in databases.[2] Subsequently complexes are assigned according to the proteins that repeatedly copurify with a particular TAP fusion protein. Direct contacts between components however are not established beyond the level of copurification, and subunit stoichiometry remains unknown. Consequently an interaction map cannot be generated, and these data sets are not readily amenable to molecular modeling.

To complement these standard proteomics methods, we are developing a MS approach in which complexes are isolated from cells and maintained intact throughout analysis. In this way, complexes retain their overall architecture, enabling us to establish not only mass spectra of intact complexes with masses up to one megadalton but also their subunit stoichiometry and interaction map. To define the subunit interactions within a complex, we use chemical cross-linking or perturbation in solution, as well as dissociation in the gas phase to generate multiple overlapping subcomplexes. Using a software package developed in house, we assign the subunit composition of these subcomplexes and determine the shortest path network that connects all subunits. To validate this approach and demonstrate the use of our software during various stages, we have used two complexes isolated from yeast, the 19S proteasome lid and the RNA exosome. Without recourse to known structural features and based on the interaction maps generated here, we extend our analysis by considering the location of homologous subunits. This enables us to refine previous models[3,4] and to generate the first atomic model for the yeast RNA exosome.

A 3D Proteomics Approach

A brief outline of the approach taken in our analysis is shown (Figure 1). The complex of interest is isolated via an affinity purification of a tagged protein, typically either a His-tagged or TAP-tagged subunit (step 1).[5] The complex-containing solution is divided into three aliquots; two aliquots are used for identifying subunits and determining the masses of the intact subunits (~4 pmol in total) and one for definition of the mass of the intact complex and generation of subcomplexes (~20 pmol total). The subunit identity is determined using standard proteomics methods, typically polyacrylamide gel electrophoresis and sequencing of tryptic peptides from excised bands (step 2).[6] The masses of the intact subunits are then determined (step 3) by recording a mass spectrum either at low pH or in the presence of organic solvents, conditions that denature the individual subunits. This is important since many proteins are extensively post-translationally modified.[7,8] The third aliquot is exchanged into a buffer compatible with electrospray in which the native state of the complex is maintained in solution (step 4).[9] Careful control of the conditions within the spectrometer is required to record a mass spectrum of the intact complex. This establishes the overall mass of the complex as well as the existence of substoichiometric interactors.

The next stage is to actively generate multiple overlapping subcomplexes (step 5) either (i) by denaturing after chemical cross-linking, (ii) by adding subdenaturing concentrations of mild denaturants, (iii) by changing the ionic strength of complex-containing solutions, or (iv) by dissociation of activated complexes in the gas phase. Cross-linked complexes are separated on a denaturing gel, and cross-linked subunits are identified using standard proteomics methods.[10] The addition of subdenaturing concentrations of organic solvents disrupts hydrophobic interfaces and consequently generates additional subcomplexes in solution. Similarly, changes in ionic strength can induce subcomplexes. Dissociation in the gas phase is used to assign subcomplexes generated in solution.

The gas-phase dissociation process involves unfolding of a peripheral subunit, released from the complex as a highly charged individual protein subunit.[11] Concomitantly, "stripped" complexes are formed with lower charge than the original complex. Practically therefore this dissociation process enables identification of at least one protein subunit. The activation of complexes in the gas phase also aids removal of associated water or buffer molecules and consequently increases the accuracy of the mass measurement over those of inactivated complexes.[12] As a final check on consistency, both masses and charges of the monomeric subunits expelled and the stripped complexes formed sum to the mass and charge of the original ion isolated for tandem MS. We also use this gas-phase dissociation process to determine the relative position of subunits, reasoning that peripheral subunits dissociate preferentially to those that make up the core.[11,13] Our assumptions are that accessibility plays a key role in determining the leaving subunit. We reason that unfolding of a core subunit is

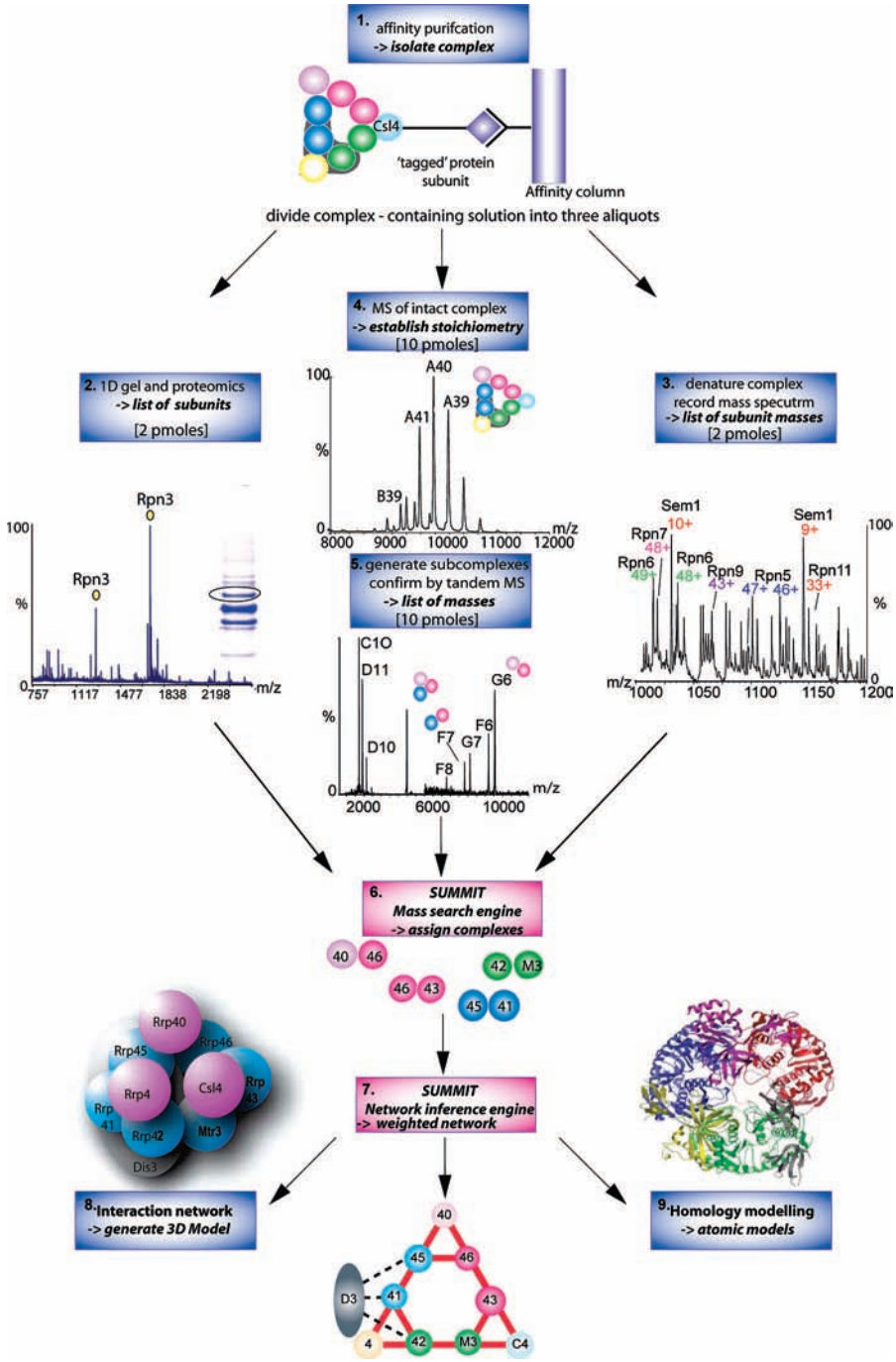

FIGURE 1. Flowchart describing the steps taken and approximate quantities of protein complex consumed and illustrated with data from the two examples described here. The complex of interest is isolated via an affinity tag and column chromatography (step 1). The subunit composition of the complex is determined using gel electrophoresis followed by tryptic digestion and MALDI TOF/TOF analysis and is illustrated for the 19S proteasome lid with peptides derived from the subunit Rpn3 (circled, step 2). A C4 ZipTip was used to exchange the complex into a low pH solution, and a spectrum of the denatured proteasome lid was used to determine the masses of intact subunits (step 3). After buffer exchange into ammonium acetate (10−1000 mM), a spectrum of the intact complex is recorded (step 4). Series A and B are assigned to the intact 10-component complex (in this case, the 400 kDa yeast exosome) and to substoichiometric binding of components, respectively. Denaturants were used to disrupt the hydrophobic core of the exosome generating a heterotrimer confirmed by tandem MS (step 5). To assign subcomplexes, masses of subunits together with their stoichiometry are submitted to SUMMIT, and the search engine is used to define possible compositions within a defined error (step 6). This list of subcomplexes is then submitted to SUMMIT for determination of an interaction network (step 7) in which the area of each subunit is scaled according to its mass and the connections are weighted according to the number of times they occur within the various networks. Red lines denote a weighted average of 1 implying that they are present in all network solutions. From this network, a 3D model for the subunit architecture may be generated (step 8), and given the availability of homologous protein structures in databases, an atomic model may be derived (step 9).

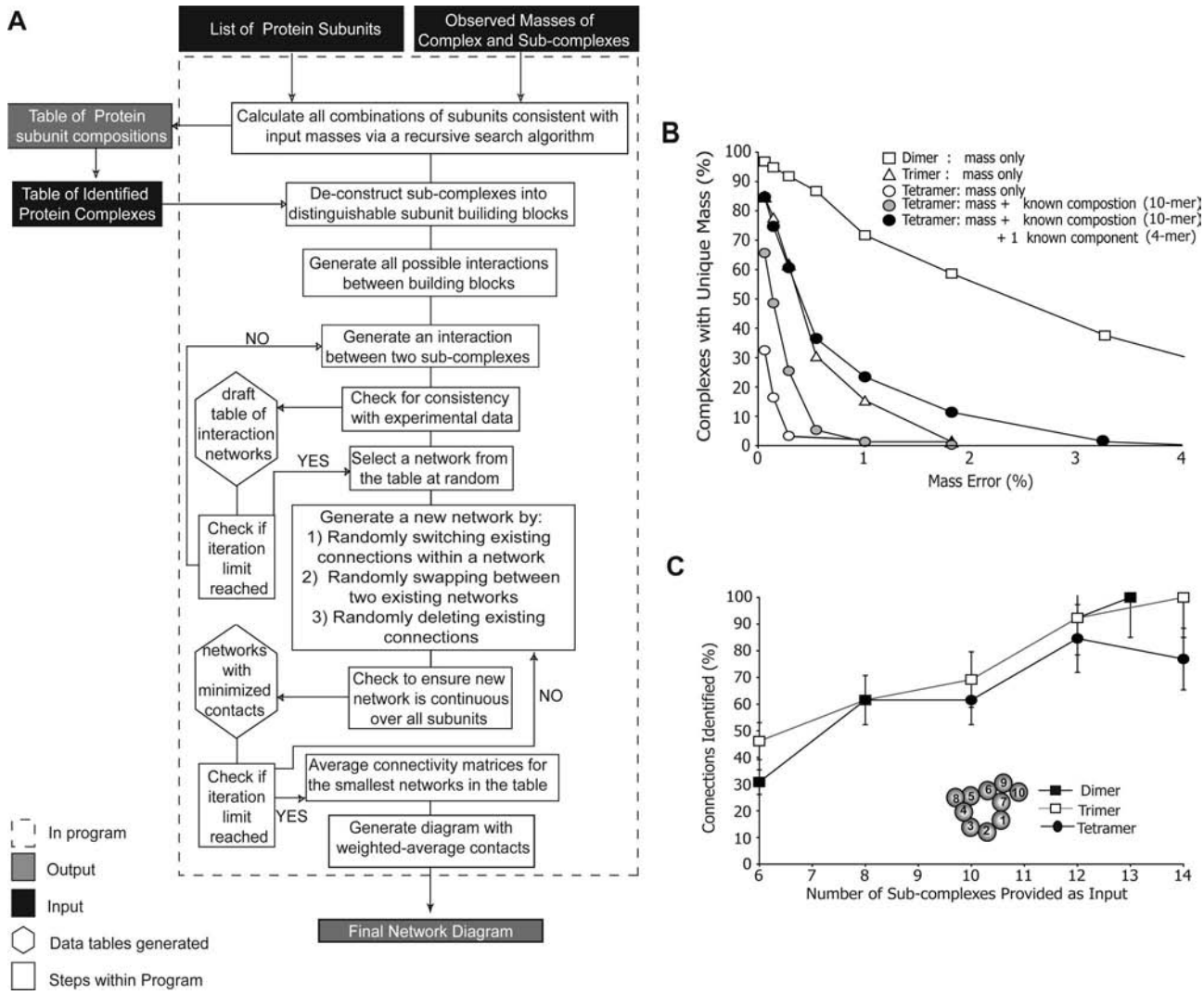

FIGURE 2. Flow diagram depicting the various stages in SUMMIT and investigation of the mass accuracy and number of subcomplexes required for our method. A list of known subunits and observed masses, together with any limiting information about their stoichiometry and tolerance in mass measurement, is submitted (panel A). A recursive algorithm defines their composition and lists all acceptable protein complexes, which are then submitted to the network algorithm. Subcomplexes are then deconstructed to generate common building blocks. Interactions between the building blocks are generated and examined for consistency with experimental data. Potential interaction networks are stored and refined by randomly switching and deleting interactions within and between networks. The output is an interaction network with connections displayed as weighted averages. To explore the mass accuracy required for our method, unique complexes, dimers (□), trimers (△) and tetramers (○), were selected at random from 100 complexes containing 6−14 subunits of unknown composition, submitted to SUMMIT, and plotted as a function of mass error (%) (panel B). Similarly tetramers with unique masses (%) selected from the 100 complexes when the overall subunit composition of the 10-mer is established (gray circles), together with one subunit identified from tandem MS (●), are plotted (panel B). To examine the number of complexes required to define interactions within a ring, a plot of connections identified (%) as a function of the number of subcomplexes submitted to SUMMIT is shown (panel C). Error bars represent the variance among five trials. A full description of the program is given in the Supporting Information.

highly unlikely since it will be stabilized by many noncovalent interactions. Our second assumption is that the activated complex retains it solution-phase subunit connectivity. Both of these assumptions are supported by a wealth of experimental data.[14]

The subunit composition of the subcomplexes generated, either in solution or in gas phases, is assigned using our software package SUMMIT (summing masses for interaction topology, step 6). The algorithm used to perform this task involves an exhaustive search for masses that sum to the target mass over all allowed stoichiometries within a given error range (Figure 2A). The output of this routine is a list of subcomplexes that can be used to build an interaction network using manual methods. However it is difficult to rule out the existence of all possible networks compatible with the subcomplexes observed. We have developed a network inference algorithm

capable of considering all possible solutions (also contained within SUMMIT, step 7). Taking a simplified approach, ignoring the 3D aspect of protein complexes and deconstructing complexes into their smallest possible protein building blocks, we then generate all viable interactions between these building blocks. Subsequently, we order according to the number of connections in each network. Our rationale is simply parsimony, that the simplest description of the contact network between proteins is most likely the correct one.

Defining the Limits of Our Approach

(i) Assigning Subcomplexes from Their Masses. One question that arises is how accurate do masses have to be to define the composition of a particular subcomplex? We use SUMMIT to investigate how mass accuracy and knowledge of the subunit composition affect our ability to define an overall topology map.

We created 100 hypothetical protein complexes, composed of between six and fourteen subunits, with a uniform distribution of masses from 10 to 50 kDa and generated sets of 100 protein dimers, trimers, or tetramers from these complexes. These were submitted to SUMMIT, and the number of unique masses within a given error limit for the different oligomers was recorded (Figure 2B). Errors of ~1% are typical for hetero-oligomeric complexes of up to 1 MDa from mass measurement alone.[12] The results show that within these error limits no tetramers and <16% and >70% of trimers and dimers, respectively, have unique masses. We can conclude therefore that it is not possible, in general, to assign subcomplexes with more than three subunits from intact mass alone.

To mimic the situation encountered in our method, we then considered 100 randomly generated tetramers examined in a tandem MS experiment. From this experiment, it is possible to achieve mass measurement errors that are much lower than those from mass spectra alone (typically 0.1%). Within this limit and given the masses and stoichiometry of all the subunits within the parent complex (e.g., from spectra of the denatured and intact protein complexes, respectively), we find that this restriction enables us to define ~55% of tetramers within an error limit of 0.1%. Knowledge of the overall subunit composition and identification of one component within the tetramer, from a tandem MS experiment, increases our definition further such that it is possible to assign >83% of tetramers. These examples highlight the necessity for tandem MS for assigning one component and reducing errors in mass measurement.

(ii) Numbers of Subcomplexes. To examine the minimum numbers of subcomplexes required to define interactions, we performed a series of experiments on networks of proteins. Two 10-mer complexes were considered: (i) a ring similar to the arrangement of the yeast exosome[4] but with seven subunits in the ring rather than six and three peripheral subunits connected to the outside of the ring and (ii) a bicluster, similar to the arrangement of the yeast 19S proteasome lid,[3] with two clusters of four or five subunits. We tested the ability of the algorithm to determine subunit contacts by randomly generating six to fourteen dimers, trimers, or tetramers from each decamer and inputting these subcomplexes into our network inference algorithm. Interactions with weighted averages greater than 0.5 present in the original complex were recorded (see Supporting Information). Similar results were obtained for the bicluster (data not shown) and the ring complex (Figure 2C). Interestingly tetrameric subcomplexes allow only ~75% accuracy at most, and increasing the number of tetramers above 12 does not improve the number of correct interactions determined. By contrast 13 dimers enable complete prediction of all interactions of the ten proteins in the ring complex. Together, these results demonstrate that dimers are most readily assigned via tandem MS and mass measurement and also the most informative for defining network connections.

To explore the use of the assignment and network algorithms during the various stages of analyses, we apply our approach to two endogenous yeast complexes isolated at natural expression levels. Although there is evidence for topological features within the two complexes selected, the 19S proteasome lid and the exosome consist of a bicluster[15] and a ring,[16] respectively, we did not include this knowledge in our analyses.

An Interaction Network for the 19S Proteasome Lid

After isolation of the 19S proteasome lid complex via a His-tagged Rpn11 subunit, the composition of the complex was validated using standard proteomics methods, and the subunit masses were established from a denatured spectrum.[3] A further aliquot was equilibrated in volatile buffer prior to analysis of the intact complex. The mass determined for the intact complex is consistent with a single copy of each of the nine subunits as well as the existence of substoichiometric binding of Rpn6 and a subcomplex consisting of four proteins (Figure 3A). Tandem MS showed that Rpn6, -9, and -12 dissociate readily from the complex. From the overall mass of the tetrameric subcomplex, there are two possible tetramers containing either Rpn5, -6, -8, and -9 or Rpn3, -7, -9, and -12 within an acceptable mass error (0.18%). To distinguish these pos-

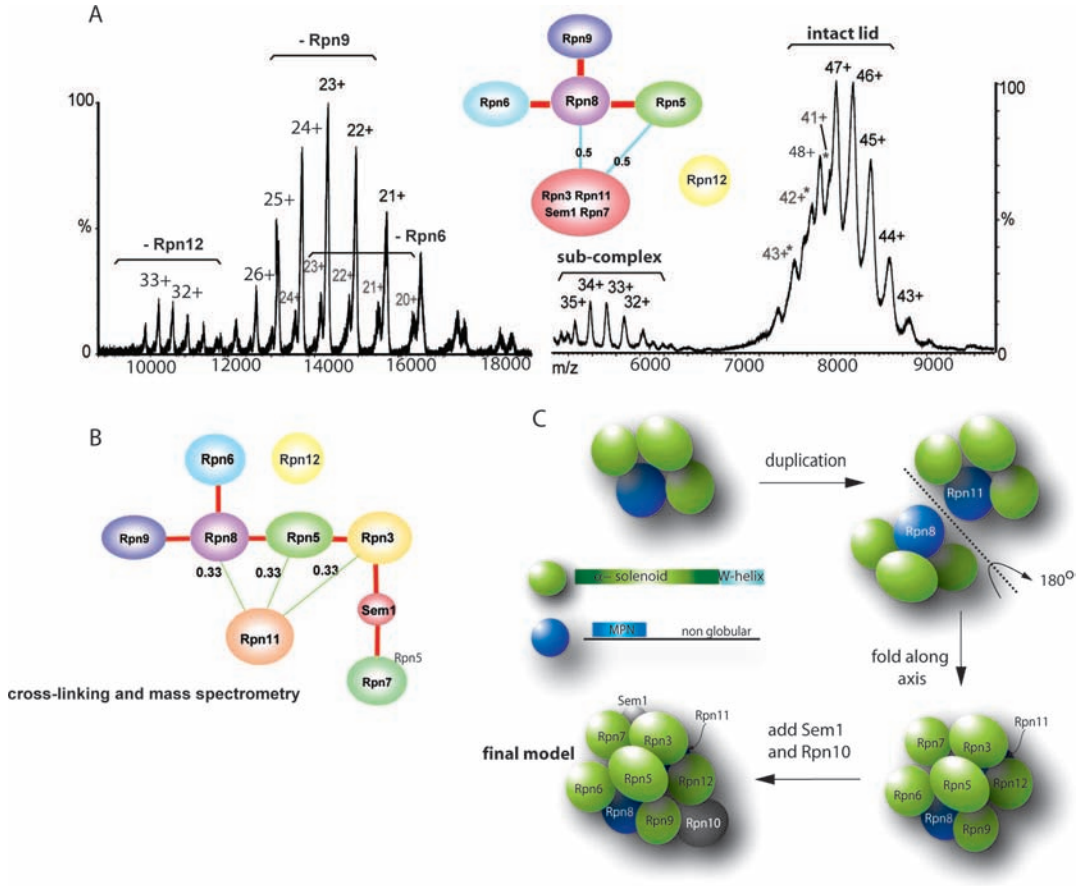

FIGURE 3. MS of the intact 19S proteasome lid, together with interaction networks generated during the analyses and the final model proposed from duplication of a tetrameric cluster. The mass spectrum of the intact lid (right-hand side) shows a major charge state series (43^+ to 48^+) and a second series assigned to an intact complex in which Rpn6 is absent (labeled $*$) (panel A). A subcomplex, charge state series (32^+ to 35^+), is assigned to a tetramer containing Rpn5, -6, -8, and -9. Tandem MS of the 47^+ charge state gives rise to individual subunits at low *m/z* (not shown) and stripped complexes between 10 000 and 18 000 *m/z* (left-hand side, panel A). These are assigned to complexes in which a single subunit has been expelled, either Rpn6, -9, or -12. From this tandem MS and that of the tetrameric subcomplex, we can generate a network that defines the peripheral subunits Rpn 5, -6, -9, and -12 and locates interactions between Rpn5 and -8 within the tetrameric subcomplex. Red lines indicate a weighted average >0.8. Four of the subunits are clustered together within the network (Rpn 3, -7, and -11 and Sem1) and cross-linking defined their interactions. Combining both data sets leads to the overall interaction network (panel B) in which interactions of 7 of the 9 subunits are placed with high confidence. Considering homologous subunits suggests that this complex may have evolved via duplication of two homologous structural lobes (panel C). Rotation to form a face-to-face conformation and interactions with Sem1, defined by cross-linking, and Rpn10, taken from yeast two-hybrid analyses,[17] complete our 3D model.

sibilities, we carried out tandem MS. Results showed that Rpn5, -6, or -9 could be dissociated readily from the complex, confirming that the complex has the composition Rpn5, -6, -9, and -8 and that Rpn5, -6, and -9 are peripheral. The interaction network produced from this data set using SUMMIT shows that we cannot define the location of Rpn3, -7, or -11 or Sem1 but that Rpn6, -5, and -9 occupy peripheral locations with Rpn8 at the center of the subcomplex (Figure 3A).

To supplement this information, we used a chemical cross-linking strategy.[10] After incubation with chemical cross-linker bis(sulphosuccinimidyl)suberate (BS3) and separation of cross-linked subunits on a 1D gel, tryptic peptides enabled us to define six different subcomplexes. In this approach, neighboring subunits are identified through comigration of cross-linked proteins and not from cross-linked peptides. Consequently binding sites within subunits are not defined, but additional subcomplexes can be characterized. The interaction network deduced from cross-linking demonstrates high-confidence interactions between Rpn3, -5, and -7 and Sem1 (all with weighted averages ≥ 0.5). Combining both data sets gives a total of 14 subcomplexes (6 from cross-linking and 8 from MS alone). Submitting these to SUMMIT yields a network in which 7 of the 9 proteins are located with high confidence (Figure 3B). The only exceptions are subunit Rpn11, which can interact with either Rpn3, -5, or -8, and subunit Rpn12, which is readily lost from the complex.

Previously, to define the locations of Rpn11 and -12, we supplemented our model[3] with data from yeast two-hybrid

analyses.[17] An alternative approach is to consider the complex in terms of homologous subunits. Initially, we predicted the fold types by sequence comparison methods. Eight of the nine subunits share considerable homology. Rpn8 and -11 contain metalloproteinase domains, while Rpn3, -5, -6, -7, -9, and -12 contain α-solenoid and W-helix motifs, often involved in protein–protein interactions. Sem1, the smallest subunit, shows no homology to proteins of known structure. Based on this consideration, the subcomplex Rpn5, -6, -8, and -9 identified in the MS experiments would form one structural lobe of the complex with Rpn8 occupying the central position. The other structural lobe would comprise Rpn3, -7, -11, and -12, in which Rpn11, the active subunit of the lid, occupies a central position analogous to that occupied Rpn8. We construct a homology-based model by rotating by 180° the subcomplex containing Rpn8, thus enabling interactions between Rpn3 and Rpn5, identified by cross-linking. To complete our model, we place the small nonhomologous subunit Sem1 in contact with Rpn3 and -7 as defined by cross-linking (Figure 3C). To orient the lid on the base of the regulatory particle, we place Rpn9 and -12 adjacent to Rpn10 from yeast two-hybrid analyses[17] (Rpn10 was not present in our preparation).

This model satisfies all of the interactions found in our topological map and the majority of the features proposed in our previous model. The major difference is in the location of Rpn11. In the symmetrical model, proposed here, Rpn11 connects Rpn3, -7, and -12. These interactions are not supported by yeast two-hybrid analyses or found in our MS analyses. However, given the prevalence of duplication inside protein complexes, such a model is satisfying from an evolutionary standpoint. Recent studies have demonstrated that about 30% of complexes determined by large-scale proteomics studies or structural biology approaches contain subunit duplications,[18,19] suggesting a prominent role for such events in complex evolution.[20] Interestingly in this model, proteins of a similar mass occupy analogous positions further supporting their origin via duplication. Overall, this example illustrates how an incomplete interaction map can be supplemented by knowledge of homologous subunits enabling the definition of the 3D subunit architecture, even though the molecular details of the interactions cannot be predicted by homology.

The Subunit Architecture of the Yeast Exosome

Isolation of the cytoplasmic form of the yeast exosome complex was carried out using three different TAP-fusion proteins (Dis3, Csl4, and Rrp41). Standard proteomics confirmed the presence of all 10 subunits, and the mass of the intact complex was consistent with each of the subunits being present as a single copy within the complex. Initially, we used tandem MS of the intact complex to reveal at least six different subcomplexes, many related by losses of the same subunit (Figure 4a–f, shaded gray). The interaction network generated from this data set suggests that five of the ten subunits are labile in the gas phase. The remaining subunits are not released, implying that they are located in the core.

To define the remaining interactions, we used subdenaturing concentrations of organic solvents. Under these conditions, three pairwise dimers (i–iii) were formed, as well as subcomplexes in which core subunits had been displaced in solution (viii–xiii). In total, 13 subcomplexes were submitted to SUMMIT (Figure 3 blue-shaded). From the interaction network generated from this data set, we find that interactions with Csl4 and Rrp4, both lost readily in the gas phase, are not well defined but that pairwise dimers enable definition of four interactions with high confidence.

If we combine the two data sets, using in total all 21 subcomplexes shown in Figure 4, we obtain the overall interaction map (panel C). This network differs from that published[4] since previously we used only those confirmed by tandem MS and constrained our solution to the ring topology defined by EM. Here we wanted to explore the use of the network in determining unknown topological features and found that we are able to define eight high-confidence interactions (weighted averages ≥ 0.5). From this network, we can place the three peripheral proteins (Csl4, Rrp4, and Rrp40), which make common interactions with Rrp43, Rrp42/41, and Rrp45/46, respectively, such that they bridge the interactions between the heterodimers. Dis3, the largest subunit, interacts with Rrp45/41 and is placed on the opposite face to the bridging subunits, from spatial constraints, allowing us to construct our final model.

Homology Modeling of the Yeast Exosome and Proteasome Lid

We aligned the yeast exosome and 19S lid proteins to those of known structure using the HHSearch suite with default parameters.[21] It was not possible to build a model of the 19S lid due to the absence of homologous proteins of known atomic structure. For the exosome, homology models for each protein subunit were obtained separately using Modeller with default parameters.[22] With these settings, models are optimized with the variable target function method with conjugate gradients. We did not attempt to increase the quality of individual subunit models by modeling them together, minimization, or molecular dynamics because the majority of prior

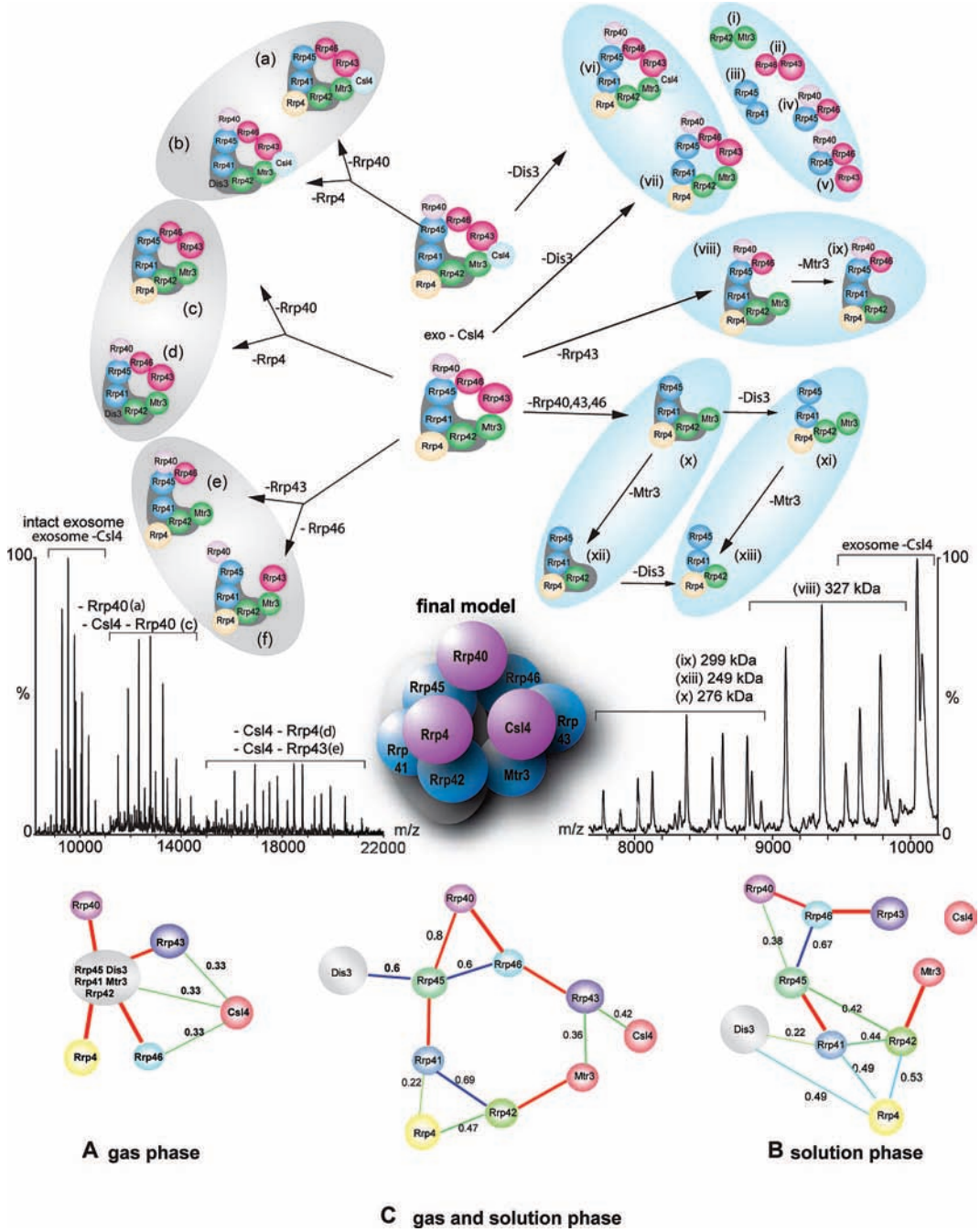

FIGURE 4. MS and subcomplexes of the yeast exosome, isolated using different tagged subunits. Spectra of the exosome subcomplexes are generated by gas-phase dissociation or disruption in solution (left- and right-hand panels, respectively). Subcomplexes generated in solution (blue) and gas phases (gray) are grouped if common subunit losses occur. The interaction network generated from the complexes formed in the gas phase defines the labile, peripheral proteins (panel A). High-confidence interactions for the pairwise dimers and the peripheral protein Rrp40 are seen in the network generated from the solution-phase data set (panel B). Incorporating both data sets leads to high-confidence interactions for the pairwise dimers, the peripheral protein Rrp40, and the ring connections, the only exception being the connection between Rrp43 and Mtr3, which is below 0.5. The peripheral proteins Csl4 and Rrp4 make fewer common interactions, but symmetry and stability of interactions around the ring imply that these subunits bridge interactions between the remaining heterodimers. Due to space constraints, we place Dis3 (gray) on the opposite face of the ring to produce our final 3D model.

research and assessment suggests that this has little effect on the quality of the model and can make models worse.[23] We found suitable templates for the three KH/S1RNA binding subunits of the exosome (Csl4, 80−292, 73% of the sequence; RRP4, 52−273, 62%; RRP40, 1−237, 99%) and the six RNase PH domain subunits (MTR3, 11−249, 96%; RRP41, 23−245, 91%; RRP46, 2−219, 98%; RRP45, 6−304, 98%; RRP43, 17−393, 96%; RRP42, 2−264, 99%). Note that models nor-

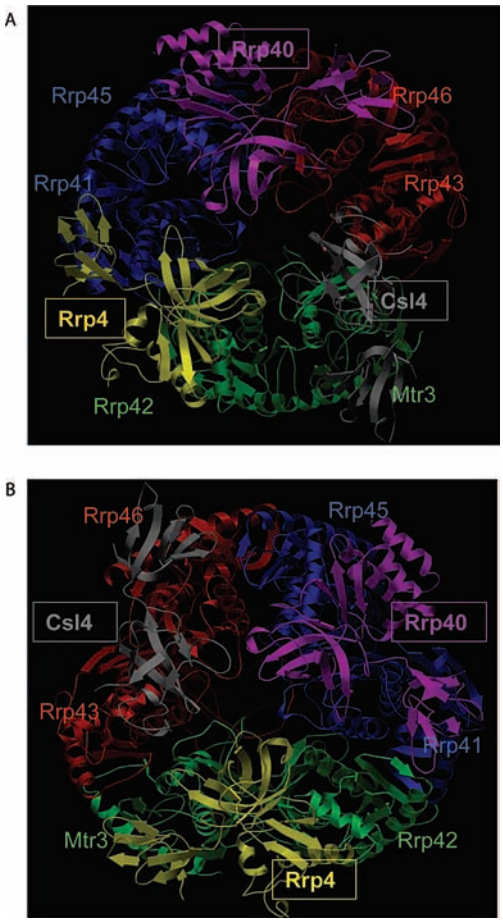

FIGURE 5. (A) Atomic models of the yeast exosome produced using the subunit interactions determined here and from structures of homologous proteins superimposed on the archaeal exosome structure PDB 2ba0. The three heterodimers that constitute the ring are shown in red (Rrp46/43), blue (Rrp41/45), and green (Rrp42/Mtr3). Bridging subunits Csl4, Rrp40, and Rrp4 are colored gray, pink, and yellow, respectively. The alternative arrangement of subunits around the ring has the bridging proteins located within the intradimer interface (model B) rather than the interdimer one. Our observations are not consistent with this model, and we conclude that panel A shows the correct atomic model of the yeast exosome.

mally constitute a fraction of the protein. Models of the proteins were superimposed on the structure of the archaeal exosome (PDB code 2ba0), using the Stamp package.[24]

Our calculated model shows clearly the complimentarity of the interactions in the intra-heterodimer interfaces and places each of the bridging subunits between the heterodimers (Figure 5A).[25] However, constraints determined by MS cannot dictate whether the ring runs clockwise or counterclockwise, meaning that one is faced with a choice of structural enantiomers. This is similar to problems with NMR, where atom−atom distances alone cannot determine, for example, whether an α-helix is left- or right-handed. In NMR, one applies the knowledge that L-amino acids can only form a left-handed helix. To select entantiomers here, one must look for similar constraints; therefore, we also modeled the alternative entantiomer (Figure 5B). The intra-heterodimer interfaces in this model are less complementary than in Figure 5A. Moreover the bridging subunits (Csl4, Rrp4, and Rrp40) are located within the intradimer interfaces rather than the interdimer interfaces as in panel A. This result is therefore not supported by our data in which these subunits bind to and strengthen interfaces between the heterodimers. Moreover, in the second model, the active sites of the catalytically active (RNase PH domain) subunits (Rrp41, Rrp46, and Mtr3) are pointing toward the bridging subunits, contrary to the known orientation of the Rrp41 equivalent in the archael exosome.[26] We conclude therefore that model A is the best fit to our experimental data and provides an atomic model of the yeast exosome and indeed agrees well with the structure of the human exosome determined recently (see below).

Conclusions and Outlook

We have demonstrated the mass accuracy and optimal numbers and sizes of subcomplexes required to distinguish two different topological arrangements of complexes. Subsequently, we applied our approach to protein complexes isolated from yeast cells at normal expression levels. For the proteasome lid, 14 complexes were deduced and submitted to SUMMIT for analysis. Of these, three were dimeric, four trimeric, and seven tetrameric or larger. The absence of multiple dimers and trimers meant that it was not possible to build a complete interaction map without using knowledge of structural motifs within subunits. For the yeast exosome, three dimers, one trimer, two tetramers, and 15 larger oligomers enabled a confident prediction of the overall architecture. Given the three heterodimers and the location of the bridging subunits, it is tempting to suggest that in the absence other structural data, we would have deduced a ring structure from our final network model.

It is of interest to compare our findings with a recent MS study of the yeast exosome[27] and an X-ray structure of the human exosome, formed by expression and reconstitution of nine subunits.[28] In the MS study, a number of subunits were found to interact only weakly with the exosome. No attempt was made to validate interactions proposed for the ring proteins[26] or their interactions with bridging subunits.[27] A number of post-translational modifications were identified, however, which, together with the 3D model proposed here, enable interesting insights into the regulation of the exosome. Six of the eight phosphorylation sites were identified on subunits Rrp46, Rrp43, Mtr3, and Csl4, all of which are located on

the labile side of the ring. This implies a possible role for phosphorylation in regulating interactions between these subunits. It is also of interest to compare the X-ray structure of the reconstituted human exosome with our model for the *in vivo* cytoplasmic form of the yeast exosome. The location of each homologous subunit is identical in our atomic model, and the structure is determined crystallographically (see Supporting Information). Minor differences are observed in some of the loops that are less structured in the model than in the X-ray structure. Similarly the C-terminal helices are shorter in the model than in the structure, because the model constitutes only a percentage of the protein sequence. Overall, however, interfaces within the ring and overall structural features are extremely well-conserved between the model and the X-ray structure.

Our model allows us to rationalize our experimental observations. The action of mild denaturants on the exosome can be explained since the surface areas of interaction are appreciably larger between the dimeric interfaces that are retained compared with those that are disrupted. Moreover the relatively low surface area of interaction calculated for Csl4 (682 $Å^2$) compared with those of the other bridging proteins Rrp40 (1292 $Å^2$) and Rrp4 (1106 $Å^2$) explains the absence of Csl4 in a large number of solution and gas-phase complexes of the yeast exosome.

In summary, this MS approach, together with the software designed to support it, holds promise for a variety of proteomic investigations. It can be used either as a stand-alone tool or in conjunction with bioinformatics and modeling to generate 3D architectures or even atomic models of protein complexes. This approach therefore advances current descriptions of complexes bringing to these lists of interactors the overall stoichiometry and presence of substoichiometric interactors, as well as interaction networks and subunit architecture. Importantly the close similarity between the X-ray structure of the human exosome and the atomic model of the yeast exosome demonstrates the potential for determining atomic models of *in vivo* complexes in advance of high-resolution structural data.

We acknowledge financial support from the EU 3D repertoire, BBSRC, Waters Kundert Trust, and the Royal Society. We thank Andrzej Dziembowski and Bertrand Séraphin for the exosome and Xavier I. Ambroggio and Raymond J. Deshaies for the 19S proteasome lid.

Supporting Information Available. A full description of the SUMMIT program and additional figures showing the comparison of the human exosome structure and the model of the yeast exosome. This material is available free of charge via the Internet at http://pubs.acs.org.

BIOGRAPHICAL INFORMATION

Tom Taverner graduated from Melbourne, Australia, and obtained his Ph.D. from Cambridge, U.K. He is currently a postdoctoral researcher at Stanford University, California.

Helena Hernández obtained her B.Sc. and Ph.D. from the University of Wales. She is currently a research associate at the University of Cambridge.

Michal Sharon received her first degree from the Hebrew University of Jerusalem and her Ph.D. at the Weizmann Institute of Science. After a postdoctoral research fellowship at Cambridge, she joined the Weizmnan Institute of Science as a senior lecturer.

Brandon T. Ruotolo obtained his B.Sc. in Chemistry from Saint Louis University in 1999 and his Ph.D from Texas A&M University in 2004. He is currently a research associate at the University of Cambridge.

Dijana-Matak Vinković received her Ph.D. in Protein Crystallography from University of Zagreb. She is currently a Research Associate at Cambridge University.

Damien Devos obtained his Ph.D. from Madrid, Spain. After postdoctoral research at the Rockefeller, NY, and UC San Francisco, CA, he is now staff at EMBL, Heidelberg, Germany.

Robert Russell obtained his Ph.D. from Oxford, U.K. After a stay at SmithKline Beecham, he is now group leader at EMBL, Heidelberg, Germany.

Carol Robinson obtained her Ph.D. from the University of Cambridge and is currently Professor of Chemical Biology in the Department of Chemistry at Cambridge.

FOOTNOTES

† This paper is dedicated to the late Dr. David Taverner (October 12, 1951 - February 11, 2008), the father of Thomas Taverner. As head of General Medicine at the Royal Adelaide Hospital his dedication to his work, patients, teaching and research, as well as his generous, gentle and modest spirit, inspired T.T. to pursue science.

REFERENCES

1 Gavin, A. C.; Aloy, P.; Grandi, P.; Krause, R.; Boesche, M.; Marzioch, M.; Rau, C.; Jensen, L. J.; Bastuck, S.; Dumpelfeld, B.; Edelmann, A.; Heurtier, M. A.; Hoffman, V.; Hoefert, C.; Klein, K.; Hudak, M.; Michon, A. M.; Schelder, M.; Schirle, M.; Remor, M.; Rudi, T.; Hooper, S.; Bauer, A.; Bouwmeester, T.; Casari, G.; Drewes, G.; Neubauer, G.; Rick, J. M.; Kuster, B.; Bork, P.; Russell, R. B.; Superti-Furga, G. Proteome survey reveals modularity of the yeast cell machinery. *Nature* **2006**, *440*, 631–636.

2 Aebersold, R.; Mann, M. Mass spectrometry-based proteomics. *Nature* **2003**, *422* (6928), 198–207.

3 Sharon, M.; Taverner, T.; Ambroggio, X. I.; Deshaies, R. J.; Robinson, C. V. Structural organization of the 19S proteasome lid - insights from MS of intact complexes. *PLoS Biol.* **2006**, *4*, 1314–1323.

4 Hernandez, H.; Dziembowski, A.; Taverner, T.; Seraphin, B.; Robinson, C. V. Subunit architecture of multimeric complexes isolated directly from cells. *EMBO Rep.* **2006**, *7* (6), 605–610.

5 Rigaut, G.; Shevchenko, A.; Rutz, B.; Wilm, M.; Mann, M.; Seraphin, B. A generic protein purification method for protein complex characterization and proteome exploration. *Nat. Biotechnol.* **1999**, *17* (10), 1030–1032.

6 Yates, J. R. r.; Gilchrist, A.; Howell, K. E.; Bergeron, J. J. Proteomics of organelles and large cellular structures. *Nat. Rev. Mol. Cell. Biol.* **2005**, *6*, 702–714.

7 Kelleher, N. L. Top-down proteomics. *Anal. Chem.* **2004**, *76*, 197A–203A.

8 Damoc, E.; Fraser, C. S.; Zhou, M.; Videler, H.; Mayeur, G. L.; Hershey, J. W.; Doudna, J. A.; Robinson, C. V.; Leary, J. A. Structural characterization of the human eukaryotic initiation factor 3 protein complex by mass spectrometry. *Mol. Cell. Proteomics* **2007**, *6*, 1135–1146.

9 Hernández, H.; Robinson, C. V. Determining the stoichiometry and interactions of macromolecular assemblies from mass spectrometry. *Nat. Protoc.* **2007**, *2*, 715–726.

10 Rappsilber, J.; Siniossoglou, S.; Hurt, E. C.; Mann, M. A generic strategy to analyze the spatial organization of multi-protein complexes by cross-linking and mass spectrometry. *Anal. Chem.* **2000**, *72* (2), 267–275.

11 Benesch, J. L.; Aquilina, J. A.; Ruotolo, B. T.; Sobott, F.; Robinson, C. V. Tandem mass spectrometry reveals the quaternary organization of macromolecular assemblies. *Chem. Biol.* **2006**, *13* (6), 597–605.

12 McKay, A. R.; Ruotolo, B. T.; Ilag, L. L.; Robinson, C. V. Mass Measurements of Increased Accuracy Resolve Heterogeneous Populations of Intact Ribosomes. *J. Am. Chem. Soc.* **2006**, *128*, 11433–11442.

13 Benesch, J. L.; Ruotolo, B. T.; Simmons, D. A.; Robinson, C. V. Protein complexes in the gas phase: Technology for structural genomics and proteomics. *Chem. Rev.* **2007**, *107* (8), 3544–3567.

14 Sharon, M.; Robinson, C. V. The Role of Mass Spectrometry in Structure Elucidation of Dynamic Protein Complexes. *Annu. Rev. Biochem.* **2007**, *76*, 167–193.

15 Fu, H.; Reis, N.; Lee, Y.; Glickman, M. H.; Vierstra, R. D. Subunit interaction maps for the regulatory particle of the 26S proteasome and the COP9 signalosome. *EMBO J.* **2001**, *20* (24), 7096–7107.

16 Aloy, P.; Bottcher, B.; Ceulemans, H.; Leutwein, C.; Mellwig, C.; Fischer, S.; Gavin, A. C.; Bork, P.; Superti-Furga, G.; Serrano, L.; Russell, R. B. Structure-based assembly of protein complexes in yeast. *Science* **2004**, *303* (5666), 2026–2029.

17 Uetz, P.; Giot, L.; Cagney, G.; Mansfield, T. A.; Judson, R. S.; Knight, J. R.; Lockshon, D.; Narayan, V.; Srinivasan, M.; Pochart, P.; Qureshi-Emili, A.; Li, Y.; Godwin, B.; Conover, D.; Kalbfleisch, T.; Vijayadamodar, G.; Yang, M.; Johnston, M.; Fields, S.; Rothberg, J. M. A comprehensive analysis of protein-protein interactions in Saccharomyces cerevisiae. *Nature* **2000**, *403* (6770), 623–627.

18 Ispolatov, I.; Yuryev, A.; Mazo, I.; Maslov, S. Binding properties and evolution of homodimers in protein-protein interaction networks. *Nucleic Acids Res.* **2005**, *33*, 3629–3635.

19 Pereira-Leal, J. B.; Levy, E. D.; Kamp, C.; Teichmann, S. A. Evolution of protein complexes by duplication of homomeric interactions. *Genome Biol.* **2007**, *8*, R51.

20 Devos, D.; Dokudovskaya, S.; Williams, R.; Alber, F.; Eswar, N.; Chait, B. T.; Rout, M. P.; Sali, A. Simple fold composition and modular architecture of the nuclear pore complex. *Proc. Natl. Acad. Sci. U.S.A.* **2006**, *103*, 2172–2177.

21 Soding, J.; Biegert, A.; Lupas, A. N. The HHpred interactive server for protein homology detection and structure prediction. *Nucleic Acids Res.* **2005**, *33* (Web Server issue), W244–W248.

22 Sali, A.; Blundell, T. L. Comparative protein modelling by satisfaction of spatial restraints. *J. Mol. Biol.* **1993**, *234*, 779–815.

23 Martin, A. C.; MacArthur, M. W.; Thornton, J. M. Assessment of comparative modeling in CASP2. *Proteins* **1997**, (Suppl 1), 14–28.

24 Russell, R. B.; Barton, G. J. Multiple protein sequence alignment from tertiary structure comparison: assignment of global and residue confidence levels. *Proteins* **1992**, *14*, 309–323.

25 Robinson, C. V.; Sali, A.; Baumeister, W. The molecular sociology of the cell. *Nature* **2007**, *450*, 973–982.

26 Lorentzen, E.; Walter, P.; Fribourg, S.; Evguenieva-Hackenberg, E.; Klug, G.; Conti, E. The archaeal exosome core is a hexameric ring structure with three catalytic subunits. *Nat. Struct. Mol. Biol.* **2005**, *12* (7), 575–581.

27 Synowsky, S. A.; van den Heuvel, R. H.; Mohammed, S.; Pijnappel, P. W.; Heck, A. J. Probing genuine strong interactions and post-translational modifications in the heterogeneous yeast exosome protein complex. *Mol. Cell. Proteomics.* **2006**, *5* (9), 1581–1592.

28 Liu, Q.; Greimann, J. C.; Lima, C. D. Reconstitution, activities, and structure of the eukaryotic RNA exosome. *Cell* **2006**, *127*, 1223–1237.